Networked Zwitterionic Durable Antibacterial Surfaces

Zixu Huang, † Sina Nazifi, † Parham Jafari, † Alamgir Karim,‡ and Hadi Ghasemi,†*

†Department of Mechanical Engineering, University of Houston, 4726 Calhoun Rd, Houston, Texas 77204-4006, United States

‡Department of Chemical and Biomolecular Engineering, University of Houston, 4726 Calhoun Rd, Houston, Texas 77204-4006, United States

KEYWORDS: Zwitterion, polyethersulfone, antibacterial, surface hydration, durability

ABSTRACT

Recently, intensive research has been conducted on the development of bacterial repelling surfaces due to the disadvantages of the conventional bactericidal leaching and contact-killing surfaces for practical application. Among these bacteria-repelling methodologies, zwitterionic polymers were widely investigated owing to its excellent non-fouling property, but its durability has limited its widespread use since most of the surfaces were developed by constructing polymer brushes via atom transfer radical polymerization (ATRP). In this study, we developed zwitterionic polymer surfaces with desirable mechanical and chemical durability for long-term use through simple blending of poly(sulfobetaine methacrylate)(PSBMA)/polyethersulfone(PES) semi-interpenetrated networked microgels with hydrophobic PES polymer matrix. Results show

that the as-prepared surfaces can efficiently induce hydration layers and thus reduce the bacterial attachment through resisting non-specific protein adsorption. The bacterial adhesion for *Escherichia coli* and *Staphylococcus aureus* was investigated under both flow and static conditions. This work has set a paradigm for developing durable antibacterial surfaces with non-fouling properties.

1. INTRODUCTION

Bacterial attachment and the subsequent biofilm formation impose a major problem in both biomedical and industrial applications, including surgical equipment[1-2], water purification system[3], food processing[4] and marine vehicles[5]. The development of antibacterial surfaces has attracted progressive interest due to the large demand on the widespread use of aseptic applications. In this scenario, various strategies have been designed to develop the antibacterial surfaces, which can be mainly divided into two subcategories: (i) Antibacterial agent releasing surfaces for killing the attached and adjacent planktonic bacteria by leaching loaded bactericidal materials[6-8]; (ii) contact-killing surfaces for destructing the cell membranes via physical cell lysis or charge disruption[9-11]. Amongst these techniques, the release of the loaded antibacterial compounds is intrinsically limited by the reservoir of the antibacterial agents, and the long-term overusing of the biocides such as antibiotics will lead to resistance issues[12-14]. On the other hand, even though these approaches can sufficiently kill the attached bacteria, the surfaces will still be contaminated by the dead bacteria debris which functions as a barrier for the approaching bacteria to attach and grow on the surfaces without contacting the biocides[9]. To address these problems, bacteria-repelling surfaces were developed to suppress the accumulation of bacteria onto the surfaces by resisting non-specific protein adsorption[15-19]. Surface hydration is widely

considered as the key to the repelling property of the surfaces; various hydrophilic materials, including poly(ethylene glycol)(PEG)[20-23], tetraethylene glycol dimethyl ether (TEGDME)[24], mannitol[25] and dextran[26] have been successfully used to achieve hydration layers via hydrogen bonding. Recently, zwitterionic polymers were intensively implemented due to their stronger binding with water through electrostatic interactions. Jiang *et al.* developed ultralow fouling surfaces with zwitterionic polymers via atom transfer radical polymerization (ATRP) for antibacterial applications, the zwitterionic polymer brushes were successfully tethered to the surfaces via both "graft-to" and "graft-from" methods[27-29]. As a result, the surfaces grafted with sulfobetaine methacrylate (SBMA) exhibited ultralow protein adsorption which can substantially hinder the bacterial attachment and the subsequent biofilm formation[30-33]. However, the zwitterionic polymer brushes synthesized via ATRP was susceptible to scratch and abrasion, which hindered the widespread use of the zwitterionic polymers[34].

Aiming at the aforementioned problems, we developed a facile procedure for developing durable zwitterionic surfaces with desirable antibacterial properties. Polyethersulfone (PES) was used as polymer matrix to enhance the durability of the zwitterionic polymers owing to its superior film-forming feature, chemical stability and mechanical property[35]. Due to the elution of the zwitterionic polymers during the use of the surfaces and the poor miscibility between the hydrophobic PES and the hydrophilic zwitterionic polymers[36], semi-interpenetrated networked microgels were synthesized to obtain an integrated structure of the PES polymer matrix and zwitterionic polymers. We anticipated the integration of the microgels and the PES polymer matrix will render the entanglement of the PES chains in the microgels with the additional polymer matrix. Both Gram-negative *E. coli* and Gram-positive *S. aureus* were used as model bacteria to assess the antibacterial properties of the surfaces. The durability of the surfaces under

harsh conditions was comprehensively evaluated with respect to anti-abrasion property and pencil hardness as well as the tolerability for acidic and alkali solutions.

2. EXPERIMENTAL SECTION

2.1 Materials

Polyethersulfone (PES, Ultrason E6020P, M_w= 58,000 g mol^{-1}) was kindly provided by BASF, Inc. [2-(Methacryloyloxy)ethyl]dimethyl-(3-sulfopropyl)ammonium hydroxide (SBMA, 95%), N, N-Methylenebisacrylamide (MBA), azobisisobutyronitrile (AIBN, 98%), dimethyl sulfoxide (DMSO, 99%) were purchased from Sigma-Aldrich, Inc. All materials were used as received without any further purification.

2.2 Synthesis of the PES/PSBMA microgels

The procedure for the synthesis of the zwitterionic microgels was illustrated in **Figure 1**. Typically, 10 g of SBMA monomer, 4 g of PES matrix, 0.2 g of AIBN thermal initiator, and 0.5 g of MBA cross-linker were mixed with 84 g of DMSO into a 250 mL round bottom three-neck flask at room temperature with mechanical stirring at 400 rpm. After the PES was fully dissolved, the reaction flask was purged with nitrogen for 30 min to remove oxygen. The cross-linking polymerization was initiated by heating at 100 °C for 24 h with continuous mechanical stirring at 400 rpm.

2.3 Preparation of the PES polymer matrix solution

16 g of PES and 84 g of DMSO were added into a 250 mL round bottom three-neck flask and heated at 70 °C for 12 h to obtain a clear polymer matrix solution. The solution was then sonicated to remove dissolved air.

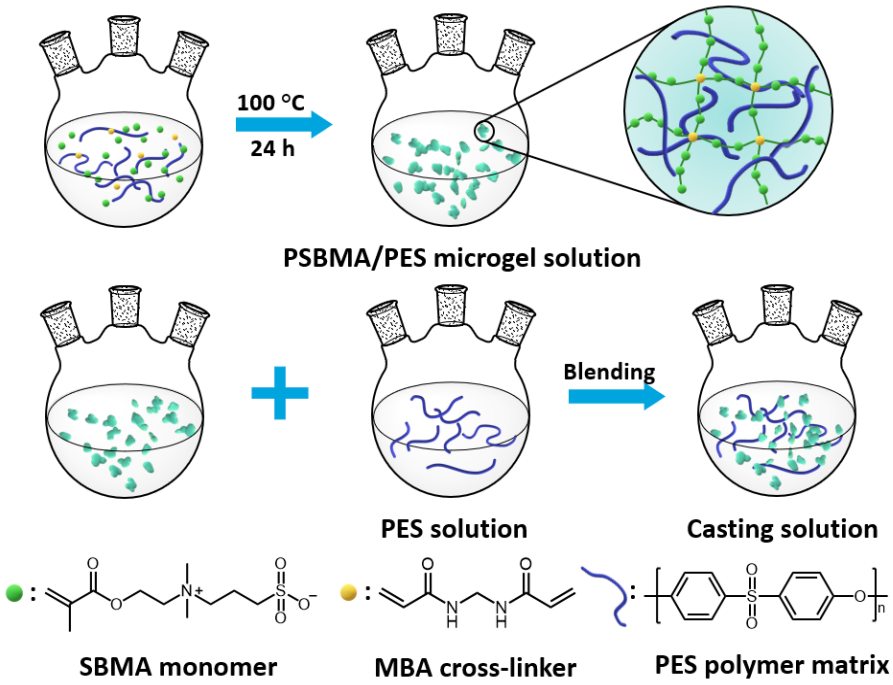

Figure 1. Synthetical route of the PES/PSBMA microgels and the preparation procedure of the casting solutions.

2.4 Preparation of the casting solution

The casting solutions were prepared by blending desired amount of the PES/PSBMA microgel solution into the PES polymer matrix solution as demonstrated in **Figure 1**. Various concentrations of the casting solution were developed as summarized in **Table 1.**

Table 1. Compositions of the casted surfaces.

Sample	PES matrix (g)	PES/PSBMA microgel (g)	Weight ratio of the microgel in the surface (%)
AB-0	1.6	0	0
AB-47	1.6	1.4	46.67
AB-64	1.6	2.8	63.64
AB-78	1.6	5.6	77.78

2.5 Preparation of the surfaces

The surfaces containing various amount of the PES/PSBMA microgels were obtained by coating the casting solutions on pre-cleaned glass (i.e. by Isopropanol solution) with a paintbrush. The surfaces prepared from different grades of the casting solutions were named as AB-0, AB-47, AB-64, and AB-78, respectively.

2.6 Bacterial culture procedure

Escherichia coli BL21 carrying a green fluorescent protein (GFP) was used as Gram-negative model bacteria for the bacterial attachment and biofilm formation assay. To start the initial culture, several colonies of *E. coli* were transferred from the stock culture to 50 mL of Miller's Luria-Bertani (LB) broth with 100 μg/mL of ampicillin using a sterile inoculation loop, the initial culture was then incubated at 37 °C with shaking at 200 rpm for 24h. The initial culture was poured into 200 mL of the LB broth to inoculate a second culture for sufficient bacterial cells. After an opaque broth was obtained, the *E. coli* cell pellets were collected by a refrigerated centrifuge at 7,500 rpm for 10 min at 4 °C and washed with sterile 0.01M PBS solution three times to remove the residual LB broth. The cell pellets were subsequently suspended in 0.01 M PBS solution at a concentration of 10^9 cells/mL and the concentration was confirmed by a UV-

Vis spectrophotometer (UV1600, VWR) by measuring the absorbance at a wavelength of 600 nm. The images of the bacteria culture and collection are depicted in **Figure S1**.

Staphylococcus aureus was utilized as a model Gram-positive bacterium for bacterial attachment assay. The culture and collection procedure are identical to the abovementioned method. The samples attached with *S. aureus* were stained with 100 μL of green fluorescent nucleic acid stain SYTO 9 (ThermoFisher, USA) and rinsed with sterile PBS solution three times for the confocal microscope imaging.

2.7 Bacterial attachment assay under static condition

To investigate the bacterial attachment biofilm formation on the surfaces under static conditions, the samples were immersed in a petri dish containing 25 mL of the *E. coli* or *S. aureus* PBS suspension with a concentration of 10^9 cells/mL. The samples were incubated for 5 h at room temperature and then washed with sterile 0.01 M PBS solution to remove the unattached and loosely-attached bacteria[37]. Afterwards, the samples were further incubated at room temperature for 12 h. Bacterial attachment properties were observed using a confocal laser scanning microscope (CLSM, Nikon Eclipse Ti-S) and the 3D images were constructed by NIS Elements AR software.

2.8 Characterization of bacterial attachment under flow condition

A parallel flow cell (BST FC284, BioSurface Technologies, Bozeman, MT) was used to characterize the bacterial attachment under flow condition. The dimension of the flow chamber is approximately 50 mm long by 13 mm wide by 2.35 mm deep. The sterile PBS suspension of bacteria with a concentration of 10^9 cells/mL was pumped through the flow cell with a syringe pump at a flow rate of 2 mL/min for 1h at room temperature, then 30 mL of the sterile LB broth

was delivered through the flow chambers at a rate of 2 mL/min for 15 min to remove the loosely-attached and incubate the attached bacteria[38-39]. Afterwards, the samples were further incubated at room temperature for 12 h. Bacterial attachment properties were observed using a confocal laser scanning microscope (CLSM, Nikon Eclipse Ti-S) and the 3D images were constructed by NIS Elements AR software.

3. RESULTS AND DISCUSSION

3.1 Morphology of the surfaces

The morphology of the surfaces was observed using scanning electron microscopy (SEM, JSM 6330F, JEOL) with an acceleration voltage of 15 kV and a working distance of 15 mm, the surfaces were deposited with 25 nm of graphite to confer electrical conductivity. As shown in **Figure 2a**,

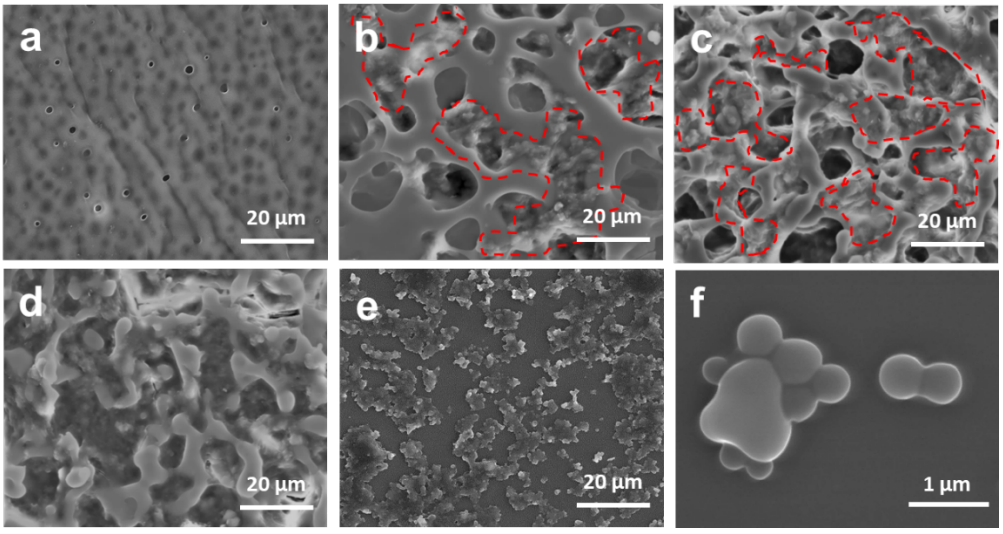

Figure 2. SEM images of the (a) AB-0 surface, (b)-(d) zwitterionic microgel modified AB-47, AB-64, and AB-78 surfaces. The zwitterionic microgels were marked by red circles. (e) and (f) zwitterionic microgels casted from PSBMA/PES solution without blending of PES solution.

pleat and wavy surface with scattered pores was observed from the pristine AB-0 surface. It was reported that the PES film possesses interconnected voids along its cross-sectional region with a skin layer on the surface[40]. After zwitterionic microgels were incorporated into the PES polymer matrix, the skin layer was no longer observed on the surface. As displayed in **Figure 2b~d**, the interconnected voids of the PES matrix were gradually filled with zwitterionic microgels, which rendered enhanced hydrophilicity and reduced roughness to the surfaces. The entanglement of the PES in zwitterionic microgels with the additional PES matrix confers desired surface integrity, thus the elution of microgels from PES matrix was circumvented when the surfaces were challenged with hydrodynamic shear force. **Figure 2e,f** shows the morphology of the films casted directly from PES/PSBMA zwitterionic microgel solution without further addition of PES matrix. A large deviation in size ranging from 300 nm to 1 μm was observed due to the agglomeration of the microgels. The insufficient film integrity confirmed blending with PES matrix is indispensable for mechanical durability.

The morphology of the surfaces was further investigated using atomic force microscopy (AFM, MultiMode 8 SPM, Bruker). The height images were scanned with ScanAsyst-Air probe. As displayed in **Figure 3a**, a relatively smooth surface was observed from AB-0 surface which is owing to the excellent film-forming property of PES. In **Figure 3b**, scattered zwitterionic microgel clusters were detected from the AB-47 surface and a surface roughness (R_q) of 58.4 nm was measured for the microgel-rich regions. For the AB-64 and AB-78 surfaces, zwitterionic microgels emerged as an integrated phase with surface roughness of 53.6 and 50.8 nm. It is inferred that the surface roughness of the microgel phase is almost independent of the content of microgel loaded into PES matrix. Therefore, higher amount of zwitterionic microgels can be utilized to construct a robust hydration layer without dramatic change of the surface morphology.

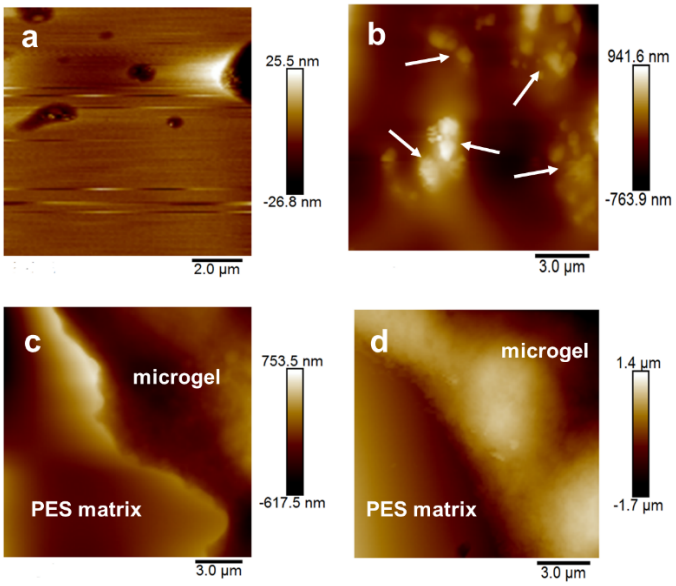

Figure 3. AFM height images of the (a) AB-0 surface, (b)-(d) zwitterionic microgel modified AB-47, AB-64, and AB-78 surfaces, respectively. The zwitterionic microgels were marked by white arrows for AB-47 surface.

3.2 Surface composition characterization

The surface chemical composition of the zwitterionic microgel modified surfaces was characterized using ATR-FTIR (Nicolet iS50, Thermo Fisher Scientific). As shown in **Figure 4a**, the peak at 1735 cm^{-1} is attributed to the stretching of the ester carbonyl group and the peak at 1032 cm^{-1} is ascribed to the sulfonate group, indicating the successful incorporation of zwitterionic microgels into the surfaces. Increased intensity of the peaks was detected from AB-47, AB-64 and AB-78 surfaces which confirmed higher content of zwitterionic microgels can be readily loaded into pristine PES surface without apparent elution during preparation process.

The chemical composition of the surfaces was further confirmed using XPS (PHI 5700, Physical Electronics). In **Figure 4b**, new signal associated with N 1s at *ca.* 400 eV and enhanced intensity of O 1s elucidated the existence of zwitterionic microgels in the surfaces. The analysis

of atomic contents was performed using XPS survey spectra and the results were summarized in **Table S1**, For the AB-78 surface, the atomic percentage of N is 4.15% which is close to the theoretical value. To investigate the chemical structure of the surfaces, high resolution XPS C 1s scan was used to characterize the chemical environment for C in both AB-0 and AB-78 surfaces. As shown in **Figure S2**, the peaks were fitted into three components of O-C=O, C-O/C-N^+, and C-C/C-H with binding energies of 288.7, 286.2, and 284.7 eV, respectively. The emergence of the O-C=O component and enhanced signal of C-O/C-N^+ further confirmed the zwitterionic microgels were successfully embedded onto the surfaces.

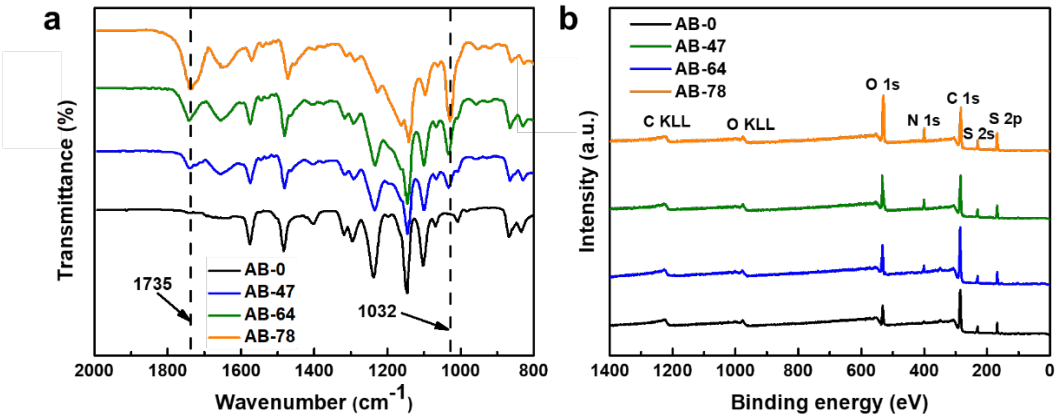

Figure 4. (a) ATR-FTIR spectra of the pristine and zwitterionic microgel modified PES surfaces. The absorption bands at 1735 cm^{-1} and 1032 cm^{-1} represent the ester carbonyl and sulfonate groups in the zwitterionic microgel; (b) XPS survey spectra of the surfaces, the signal at 400 eV is attributed to the N in the zwitterionic microgels.

3.3 Characterization of surface hydrophilicity and hydration layer

The surface hydrophilicity was characterized with a home-built contact angle goniometer equipped with CCD camera, the water contact angles (WCA) were measured using ImageJ software. Briefly, 3 μL of DI water was pipetted onto the surfaces then the images were recorded

after 5 min. As a result, the WCA of the pristine AB-0 surface was 83.6 ±6.5°. After the zwitterionic microgels were introduced, the WCAs precipitously decreased to 48.1 ±5.2°, 40.9 ±3.5°, and 25.8 ±4.6° for the AB-47, AB-64, and AB-78 surfaces, respectively. The improved wettability illustrated the strong interaction between the surfaces and water, which is attributed to the superhydrophilicity of the PSBMA polymer in the microgels.

To examine the hydration layers on the surfaces, ATR-FTIR spectroscopy was used to exclusively observe the O-H stretching bands ranging from 3000-3600 cm^{-1}. The dried surface was prepared by coating the casting solution on glass substrates, then transferred into a vacuum chamber at 80 °C for 48 h to remove the solvent. The dried sample was stored with 4 Å molecular sieve until measured. The hydrated surface was prepared from the fully dried sample, followed by the transferring into an environmental chamber with a relative humidity of 75% at 25 °C for 48 h. **Figure 5b** depicts the ATR-FTIR spectra for the dried and hydrated surfaces, respectively. It was found that the band at *ca.* 3280 cm^{-1} is attributed to the strongly bonded water on the surfaces, which can be considered as the first hydration layer. The band at 3430 cm^{-1} is commonly ascribed to the free bulk water on top of the first hydration layer. Also, the electrolyte-responsive nature of PSBMA affects thickness of hydration layer and could help on anti-fouling characteristics. In the presence of alkaline solutions, the PSBMA chains could extend longer leading to thicker hydration layers.

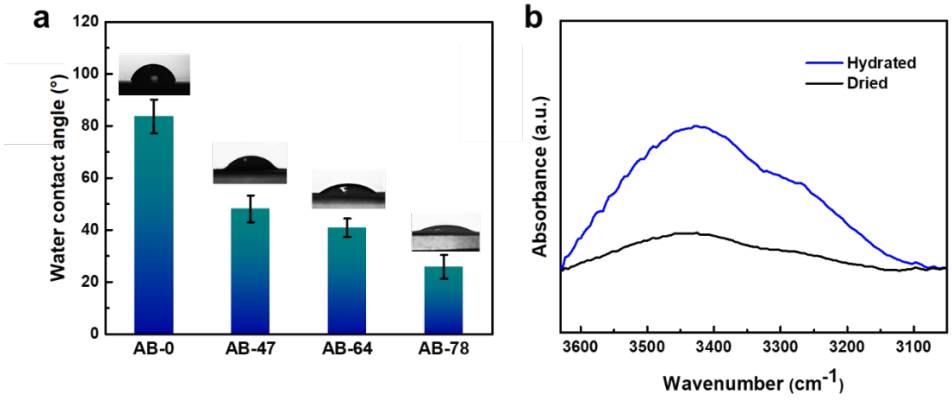

Figure 5. (a) Water contact angles for the pristine and zwitterionic microgel modified surfaces. (b) ATR-FTIR spectra of the O-H stretching vibration range for both dried and humid air hydrated AB-78 surfaces.

3.2 Bacterial attachment under static condition

To study the antibacterial properties of the surfaces, we investigated the biofilm formation of *E. coli* and *S. aureus* on the surfaces with confocal laser scanning microscopy (CLSM)[41]. **Figure 6a** shows the structure of the biofilms on surfaces incubated at room temperature for 12 h after static bacterial attachment. As a result, the pristine surface was almost fully occupied by thick biofilm layers owing to the hydrophobicity of PES, the non-specific adsorption of protein facilitated the settlement and growth of the bacteria onto the surfaces. As for the zwitterionic microgel modified surfaces, grass lawn-like biofilms were suppressed to small and scattered spots, which is owing to

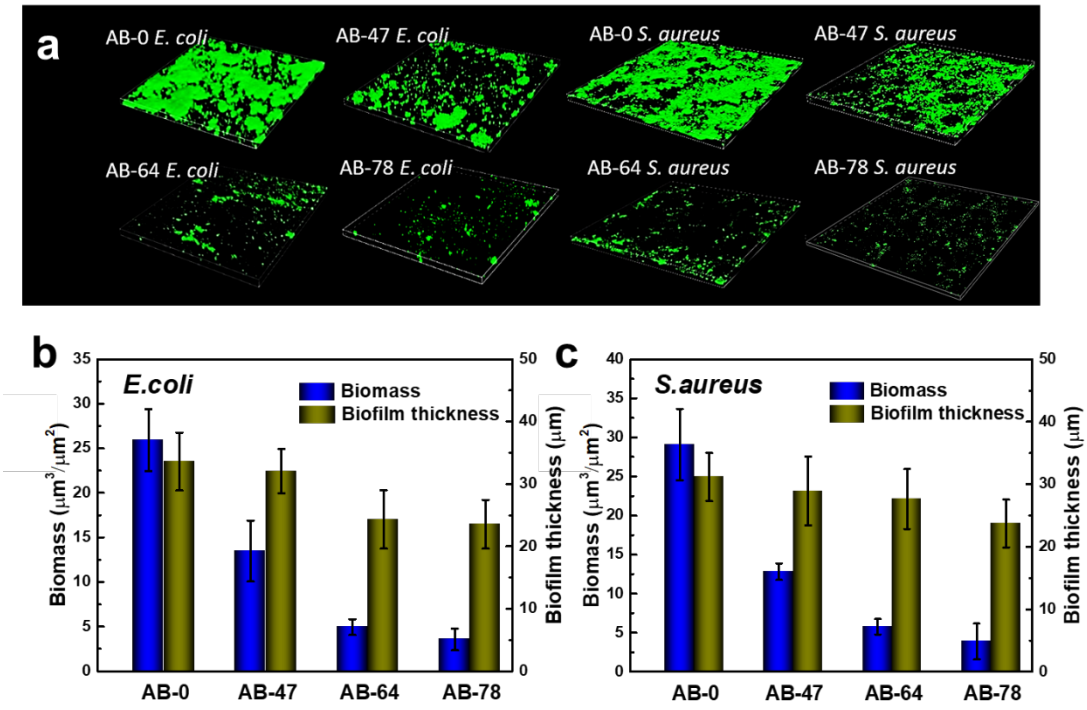

Figure 6. (a) 3D structures of the *E. coli* and *S. aureus* biofilms formed on the surfaces after bacterial attachment under static condition. The dimension of the detected regions is 400 ×400 μm. (b) and (c) quantification of the biomass and thickness of the biofilms for AB-0, AB-47, AB-64 and AB-78 surfaces, respectively.

the presence of the hydration layers. The biomass and biofilm thickness of *E. coli* adhered onto AB-78 surface were diminished from 25.92 to 3.54 $\mu m^3/\mu m^2$ and from 33.6 to 23.55 μm compared with AB-0 surface, respectively. A similar decrease in the biofilm formation of Gram-positive *S. aureus* bacterium was also observed, the biomass and biofilm thickness of AB-78 surface were reduced from 29.08 to 3.88 $\mu m^3/\mu m^2$ and from 31.18 to 23.74 μm compared with the pristine surface. These results illustrated the modified surfaces were versatile towards resisting the attachment of bacteria and the subsequent formation of biofilms for both Gram-positive and Gram-negative bacteria.

3.3 Bacterial attachment under flow condition

To further study the bacterial attachment to the surfaces under flow condition, the pristine and modified surfaces were continuously challenged with shear flow of bacteria suspension. **Figure 7** displayed the biofilm structures detected from the surfaces after incubation at room temperature overnight. As a result, more continuous biofilms were observed under flow condition compared with static condition since the earlier attached bacteria can functionalize as physical obstruction to facilitate the planktonic bacteria to adhere to the surfaces. Consequently, reduced biomass in the biofilms of AB-78 surface was observed for the flow condition than the static counterpart where the loosely attached bacteria can be readily removed by hydrodynamic shear force. These results illustrated the zwitterionic microgel modified surfaces can effectively resist bacterial attachment under shear flow, which demonstrated its potential for pipeline and underwater device applications.

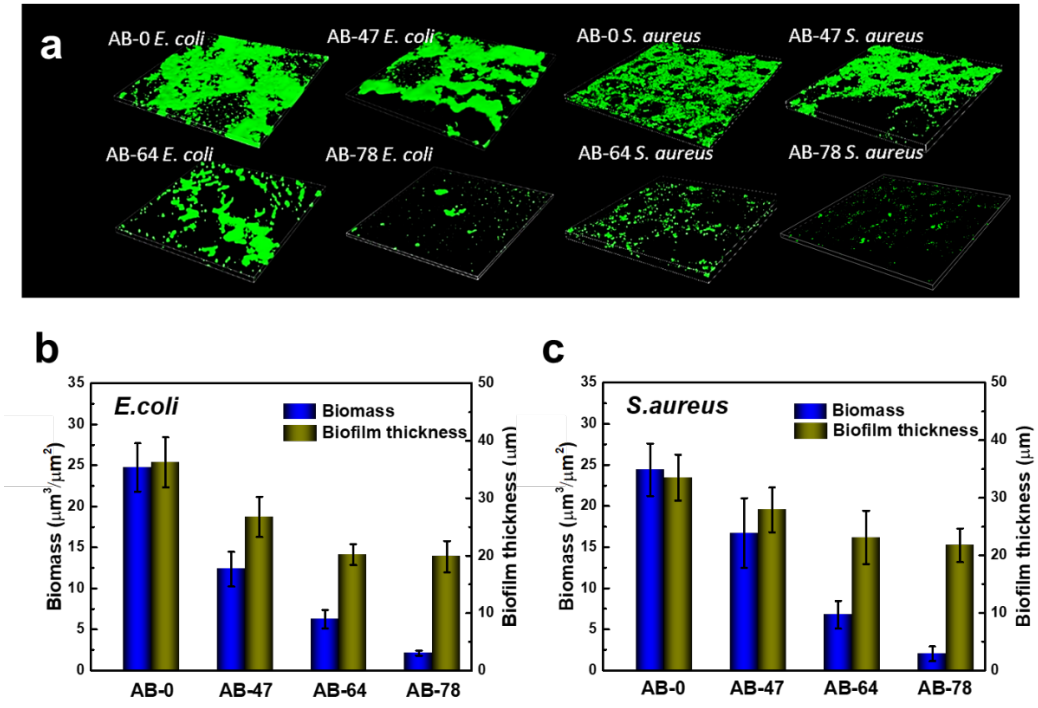

Figure 7. (a) 3D structures of the *E. coli* and *S. aureus* biofilms formed on surfaces under flow condition. The dimension of the observed regions is 400 ×400 μm; (b) and (c) quantification of the biomass and thickness of the biofilms for AB-0, AB-47, AB-64 and AB-78 surfaces, respectively.

3.3 Mechanical durability test

To assess the feasibility of practical application of the surfaces, the mechanical durability was assessed with respect to the anti-abrasion property and pencil hardness. We performed anti-abrasion test on the surfaces using a reciprocating abraser (Model 5900, Taber Industries) in accordance with ASTM D4060 standard. Briefly, the samples were tested with an abrasive tip loaded with 1N, 2.5N, and 5N abrasion forces for 1000 cycles with a stroke speed of 30 cycles per minute, the abrasion test setup was shown in **Figure 8a**. The anti-abrasion property was thus evaluated by measuring the thickness loss of the surfaces with a stylus profilometer (Alpha-Step 200, Tencor)[42-45]. As shown in **Figure 8b**, a maximum thickness loss of *ca.* 108 μm was observed from AB-78 surface which demonstrated desired anti-abrasion property. ATR-FTIR spectra were measured to confirm the chemical composition of the abraded surfaces. In **Figure 8c**, the absorption bands at 1032 and 1735 cm^{-1} which associated with sulfonate and ester groups in the zwitterionic microgels were detected for the samples after abrasion test, illustrating the zwitterionic microgels were successfully embedded throughout the vertical direction of the surfaces, no significant change in the concentration of the microgels was observed compared with pristine surface.

The surface hydrophilicity of AB-78 surface after abrasion test was characterized by measuring water contact angle on the abraded region. As summarized in **Figure 8d**, a maximum WCA of

32.46 ±4.94° was obtained from 5N abrasion load which is slightly increased from 25.84 ±4.61° of the pristine surface. The resisting property against bacteria adhesion was quantitatively analyzed by the previous methods, the biomass of both pristine and tested surfaces was compared in **Figure 8e**, sufficient antibacterial property was still observed even for the most challenging scenario. The surface hardness was measured by the pencil hardness test to confirm the surfaces for high-touch use. Concisely, the surfaces were scratched with pencils of various

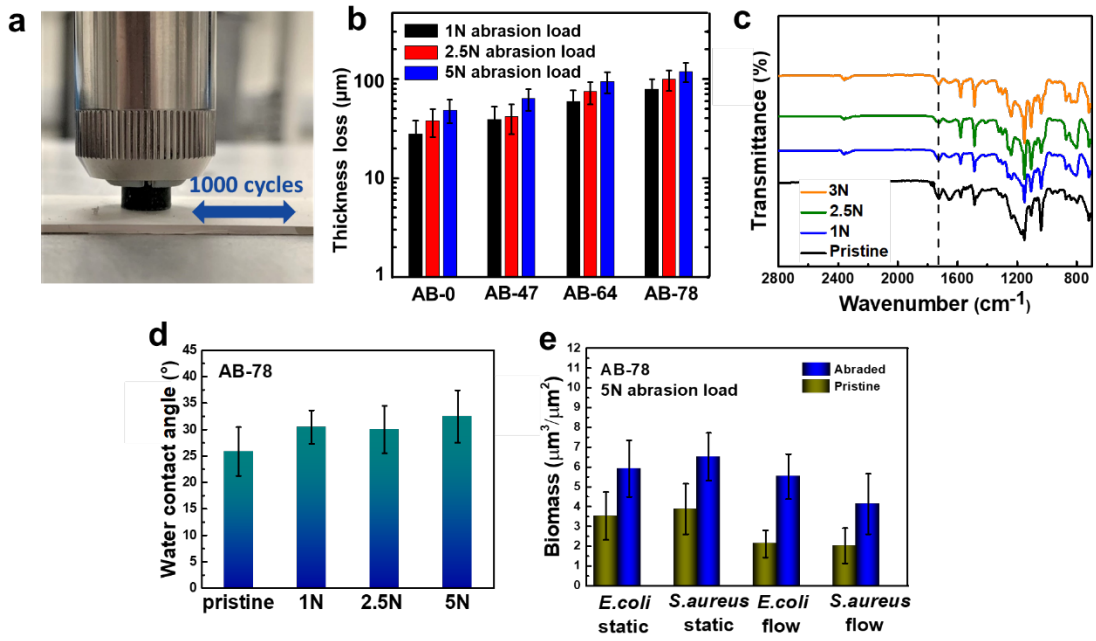

Figure 8. (a) Photo of the abrasive tip of the reciprocating abraser, the abrasion direction is indicated by the blue arrow; (b) thickness loss of the surfaces under abrasion loads of 1 N, 2.5 N and 5 N; (c) ATR-FTIR spectra for the pristine and abraded AB-78 surfaces; (d) water contact angles (WCAs) for the pristine and abraded AB-78 surfaces; (e) the biomass of the biofilms on both pristine and abraded AB-78 surfaces.

hardness ranging from 6H to 6B with a load of 750 g (ASTM D3363)[46-48], the test setup is shown in **Figure S3**. As a result, hardness ratings of 3H, HB, 2B and 3B were obtained from AB-0, AB-47, AB-64, and AB-78 surfaces, respectively. Specifically, the 4B pencil failed to cause any

obvious indentation or cohesive fracture on the most vulnerable AB-78 surface, pencil with 3B hardness rating only made few notches along the scratch direction.

3.4 Chemical durability test

The durability of the antibacterial surfaces upon exposure to harsh chemical environments was examined by immersing the as-prepared samples into acidic and alkali solutions. Briefly, concentrated hydrochloric acid was diluted to prepare acidic solutions with pH values of 2.49 and 5.83, alkali solutions with pH values of 11.76 and 13.07 were also prepared gravimetrically by dissolving sodium hydroxide in DI water. The AB-78 surface was then immersed in these solutions for 48 h at room temperature, followed by washing with DI water three times to remove excess acid and base[47, 49]. As a result, no significant change in color was observed from the samples and the testing solutions (**Figure 9a**). The chemical compositions of the AB-78 surface tested under various pH values were investigated with ATR-FTIR. In **Figure 9b,** no significant change in the intensity of the peaks at 1735 cm^{-1} and 1032 cm^{-1} was detected, indicating the excellent chemical inertness of the zwitterionic microgel towards acid and alkali. The wettability of the tested surfaces was assessed by measuring water contact angle. As shown in **Figure 9c**, all tested surfaces showed contact angles under 35°, which elucidated the surfaces can still construct hydration layer upon exposure to harsh chemical conditions. The antibacterial property of the acidic and alkali solutions treated surfaces was compared with pristine surface in **Figure 9d,e**. The biofilm formation can be sufficiently suppressed even when the surfaces were challenged with harsh chemical conditions for 48 h, the tested surfaces exhibited a maximum biomass of ca. 5.5 $\mu m^3/\mu m^2$, which is still competent for practical application. The CLSM images of the biofilms formed on the AB-78 surfaces after chemical durability test were shown in **Figure S4**.

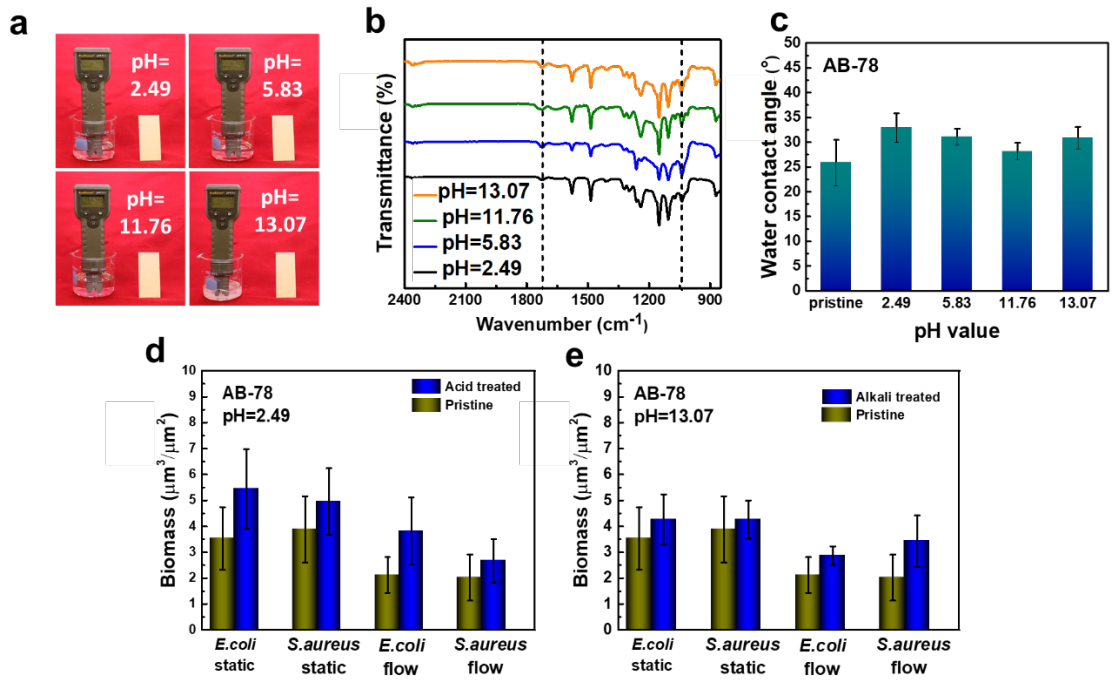

Figure 9. (a) Photos of the AB-78 surfaces tested with acidic and alkali solutions, the pH values of the testing solution were indicated by the pH meter; (b) ATR-FTIR spectra for the AB-78 surfaces after chemical stability test, dashed lines denoted the ester carbonyl and sulfonate groups in the zwitterionic microgels retained in the surfaces; (c) water contact angles for the AB-78 surface after chemical durability test; (d)~(e) the biomass in the biofilms on both pristine and tested AB-78 surfaces.

4. **CONCLUSIONS**

In this study, we implemented the idea of increasing the mechanical and chemical durability of zwitterionic polymers by blending networked zwitterionic microgels with PES polymer matrix. The zwitterionic microgels were integrated with porous PES matrix via entanglement of PES in the microgels and the additional PES matrix. The antibacterial property was conferred by the hydrophilicity of the zwitterionic polymers, surface hydration layers were thus constructed via

electrostatic interaction of the zwitterionic microgels with water. Reduced bacterial attachment and biofilm formation were observed for both Gram-negative *E. coli* and Gram-positive *S. aureus* bacteria. It was found that, thick and continuous biofilms can be sufficiently suppressed into small and scattered biofouling spots. Moreover, the mechanical durability with respect to anti-abrasion property and chemical resistance for acidic and alkali solutions had demonstrated the feasibility of applications for rigorous conditions. The zwitterionic microgels modified surfaces retained desired antibacterial property even when challenged with harsh chemical environments. These durable surfaces offer a new paradigm for practical anti-bacterial applications.

ASSOCIATED CONTENTS

Supporting Information

The Supporting Information is available free of charge on the ACS Publications website at DOI: 10.1021/acsabm.xxxxxx.

Photos of *E. coli* LB broth culture and PBS buffer suspension, high resolution XPS C 1s core level spectra, photos for the pencil hardness test, CLSM images for biofilms formed on AB-78 surfaces after mechanical and chemical durability test, EDS spectra for the AB-78 surface, ATR-FTIR spectra for the pristine concentrated acid tested AB-78 surfaces, TGA curves for the AB-0 and AB-78 surfaces, and atomic contents of the surfaces analyzed by XPS survey spectra (DOCX).

AUTHOR INFORMATION

Corresponding Author

*E-mail: hghasemi@uh.edu.

Notes

The authors declare no conflict of interest.

ACKNOWLEDGMENTS

The authors gratefully acknowledge funding support from National Science Foundation (Grant NSF- 1804204) and Natick Program (Grant W911QY-19-9-0011). We thank Bahareh Eslami for her help early in this project and Masoumeh Nazari for the characterization of surface morphology with AFM. Z. H. thanks Mr. Tian Tong in Dr. Jiming Bao's group at University of Houston for the measurement of FTIR spectra. The authors thank Ms. Sarah Hannusch and Mr. Parsa Alizadeh for the development of the antibacterial surfaces.

REFERENCES

(1) Monteiro, D. R.; Gorup, L. F.; Takamiya, A. S.; Ruvollo-Filho, A. C.; de Camargo, E. R.; Barbosa, D. B. The Growing Importance of Materials That Prevent Microbial Adhesion: Antimicrobial Effect of Medical Devices Containing Silver. Int. J. Antimicrob. Agents **2009**, 34(2), 103-110.

(2) Zegans, M. E.; Becker, H. I.; Budzik, J.; O'Toole, G. The Role of Bacterial Biofilms in Ocular Infections. DNA Cell Biol. **2002**, 21(5-6), 415-420.

(3) Li, Q.; Mahendra, S.; Lyon, D. Y.; Brunet, L.; Liga, M. V.; Li, D.; Alvarez, P. J. Antimicrobial Nanomaterials for Water Disinfection and Microbial Control: Potential Applications and Implications. *Water Res.* **2008,** *42(18)*, 4591-4602.

(4) Wong, A. C. L. Biofilms in Food Processing Environments. *J. Dairy Sci.* **1998,** *81(10)*, 2765-2770.

(5) Yu, Q.; Wu, Z.; Chen, H. Dual-Function Antibacterial Surfaces for Biomedical Applications. *Acta Biomater.* **2015,** *16,* 1-13.

(6) Kaur, R.; Liu, S. Antibacterial Surface Design–Contact Kill. *Prog. Surf. Sci.* **2016,** *91(3)*, 136-153.

(7) Gallón, S. M. N.; Alpaslan, E.; Wang, M.; Larese-Casanova, P.; Londoño, M. E.; Atehortúa, L.; Pavón, J. J.; Webster, T. J. Characterization and Study of the Antibacterial Mechanisms of Silver Nanoparticles Prepared with Microalgal Exopolysaccharides. *Mater. Sci. Eng. C* **2019,** *99,* 685-695.

(8) Tran, P. A.; O'Brien-Simpson, N.; Palmer, J. A.; Bock, N.; Reynolds, E. C.; Webster, T. J.; Deva, A.; Morrison, W. A.; O'Connor, A. J. Selenium Nanoparticles as Anti-Infective Implant Coatings for Trauma Orthopedics against Methicillin-Resistant Staphylococcus Aureus and Epidermidis: In Vitro and in Vivo Assessment. *Int. J. Nanomedicine* **2019,** *14,* 4613-4624.

(9) Cloutier, M.; Mantovani, D.; Rosei, F. Antibacterial Coatings: Challenges, Perspectives, and Opportunities. *Trends Biotechnol.* **2015,** *33(11)*, 637-652.

(10) Reed, J. H.; Gonsalves, A.; Roman, J.; Oh, J.; Cha, H.; Dana, C.; Toc, M.; Hong, S.; Hoffman, J. B.; Andrade, J. E. Ultra-Scalable Multifunctional Nanoengineered Copper and

Aluminum for Anti-Adhesion and Bactericidal Applications. *ACS Appl. Bio Mater.* **2019,** 2, 7, 2726-2737.

(11) Bassous, N. J.; Jones, C. L.; Webster, T. J. 3-D Printed Ti-6al-4v Scaffolds for Supporting Osteoblast and Restricting Bacterial Functions without Using Drugs: Predictive Equations and Experiments. *Acta Biomater.* **2019,** 96, 662-673.

(12) Hasan, J.; Crawford, R. J.; Ivanova, E. P. Antibacterial Surfaces: The Quest for a New Generation of Biomaterials. *Trends Biotechnol.* **2013,** *31(5)*, 295-304.

(13) Llor, C.; Bjerrum, L. Antimicrobial Resistance: Risk Associated with Antibiotic Overuse and Initiatives to Reduce the Problem. *Ther. Adv. Drug Saf.* **2014,** *5(6)*, 229-241.

(14) Weinstein, R. A. Controlling Antimicrobial Resistance in Hospitals: Infection Control and Use of Antibiotics. *Emerg. Infect. Dis.* **2001,** *7(2)*, 188.

(15) Wei, T.; Tang, Z.; Yu, Q.; Chen, H. Smart Antibacterial Surfaces with Switchable Bacteria-Killing and Bacteria-Releasing Capabilities. *ACS Appl. Mater. Interfaces* **2017,** *9(43)*, 37511-37523.

(16) Banerjee, I.; Pangule, R. C.; Kane, R. S. Antifouling Coatings: Recent Developments in the Design of Surfaces That Prevent Fouling by Proteins, Bacteria, and Marine Organisms. *Adv. Mater.* **2011,** *23(6)*, 690-718.

(17) Razavi, S. M. R.; Oh, J.; Haasch, R. T.; Kim, K.; Masoomi, M.; Bagheri, R.; Slauch, J. M.; Miljkovic, N. Environment-Friendly Anti-Biofouling Superhydrophobic Coatings. *ACS Sustain. Chem. Eng.* **2019**, 7, 17, 14509-14520.

(18) Stark, A. Y.; Mitchell, C. T. Stick or Slip: Adhesive Performance of Geckos and Gecko-Inspired Synthetics in Wet Environments. *Integr. Comp. Biol.* **2019**, 59 (1)-214-226.

(19) Garner, A. M.; Stark, A. Y.; Thomas, S. A.; Niewiarowski, P. H. Geckos Go the Distance: Water's Effect on the Speed of Adhesive Locomotion in Geckos. *J. Herpetol.* **2017,** *51(2)*, 240-244.

(20) Joseph, C. A.; McCarthy, C. W.; Tyo, A. G.; Hubbard, K. R.; Fisher, H. C.; Altscheffel, J. A.; He, W.; Pinnaratip, R.; Liu, Y.; Lee, B. P. Development of an Injectable Nitric Oxide Releasing Poly (Ethylene) Glycol-Fibrin Adhesive Hydrogel. *ACS Biomater. Sci. Eng.* **2018,** *5(2)*, 959-969.

(21) Pinnaratip, R.; Meng, H.; Rajachar, R. M.; Lee, B. P. Effect of Incorporating Clustered Silica Nanoparticles on the Performance and Biocompatibility of Catechol-Containing Peg-Based Bioadhesive. *Biomed. Mater.* **2018,** *13(2)*, 025003.

(22) Li, Y.; Meng, H.; Liu, Y.; Narkar, A.; Lee, B. P. Gelatin Microgel Incorporated Poly (Ethylene Glycol)-Based Bioadhesive with Enhanced Adhesive Property and Bioactivity. *ACS Appl. Mater. Interfaces* **2016,** *8(19)*, 11980-11989.

(23) Liu, Y.; Meng, H.; Konst, S.; Sarmiento, R.; Rajachar, R.; Lee, B. P. Injectable Dopamine-Modified Poly (Ethylene Glycol) Nanocomposite Hydrogel with Enhanced Adhesive Property and Bioactivity. *ACS Appl. Mater. Interfaces* **2014,** *6(19)*, 16982-16992.

(24) Cao, L.; Chang, M.; Lee, C. Y.; Castner, D. G.; Sukavaneshvar, S.; Ratner, B. D.; Horbett, T. A. Plasma-Deposited Tetraglyme Surfaces Greatly Reduce Total Blood Protein Adsorption,

Contact Activation, Platelet Adhesion, Platelet Procoagulant Activity, and in Vitro Thrombus Deposition. *J Biomed. Mater. Res. A* **2007,** *81(4)*, 827-837.

(25) Luk, Y.-Y.; Kato, M.; Mrksich, M. Self-Assembled Monolayers of Alkanethiolates Presenting Mannitol Groups Are Inert to Protein Adsorption and Cell Attachment. *Langmuir* **2000,** *16(24)*, 9604-9608.

(26) McArthur, S. L.; McLean, K. M.; Kingshott, P.; St John, H. A.; Chatelier, R. C.; Griesser, H. J. Effect of Polysaccharide Structure on Protein Adsorption. *Colloids Surf. B Biointerfaces* **2000,** *17(1)*, 37-48.

(27) Jiang, S.; Cao, Z. Ultralow-Fouling, Functionalizable, and Hydrolyzable Zwitterionic Materials and Their Derivatives for Biological Applications. *Adv. Mater.* **2010,** *22(9)*, 920-932.

(28) Zhang, Z.; Vaisocherová, H.; Cheng, G.; Yang, W.; Xue, H.; Jiang, S. Nonfouling Behavior of Polycarboxybetaine-Grafted Surfaces: Structural and Environmental Effects. *Biomacromolecules* **2008,** *9(10)*, 2686-2692.

(29) Li, G.; Cheng, G.; Xue, H.; Chen, S.; Zhang, F.; Jiang, S. Ultra Low Fouling Zwitterionic Polymers with a Biomimetic Adhesive Group. *Biomaterials* **2008,** *29(35)*, 4592-4597.

(30) Cheng, G.; Zhang, Z.; Chen, S.; Bryers, J. D.; Jiang, S. Inhibition of Bacterial Adhesion and Biofilm Formation on Zwitterionic Surfaces. *Biomaterials* **2007,** *28(29)*, 4192-4199.

(31) Yue, W.-W.; Li, H.-J.; Xiang, T.; Qin, H.; Sun, S.-D.; Zhao, C.-S. Grafting of Zwitterion from Polysulfone Membrane Via Surface-Initiated Atrp with Enhanced Antifouling Property and Biocompatibility. *J. Membr. Sci.* **2013,** *446,* 79-91.

(32) Chiang, Y.-C.; Chang, Y.; Higuchi, A.; Chen, W.-Y.; Ruaan, R.-C. Sulfobetaine-Grafted Poly (Vinylidene Fluoride) Ultrafiltration Membranes Exhibit Excellent Antifouling Property. *J. Membr. Sci.* **2009,** *339(1-2)*, 151-159.

(33) Kuang, J.; Messersmith, P. B. Universal Surface-Initiated Polymerization of Antifouling Zwitterionic Brushes Using a Mussel-Mimetic Peptide Initiator. *Langmuir* **2012,** *28(18)*, 7258-7266.

(34) Wang, W.; Lu, Y.; Xie, J.; Zhu, H.; Cao, Z. A Zwitterionic Macro-Crosslinker for Durable Non-Fouling Coatings. *Chem. Commun. (Camb.)* **2016,** *52(25)*, 4671-4674.

(35) Cheng, C.; Li, S.; Zhao, W.; Wei, Q.; Nie, S.; Sun, S.; Zhao, C. The Hydrodynamic Permeability and Surface Property of Polyethersulfone Ultrafiltration Membranes with Mussel-Inspired Polydopamine Coatings. *J. Membr. Sci.* **2012,** *417,* 228-236.

(36) Kim, J.; Kim, C. Ultrafiltration Membranes Prepared from Blends of Polyethersulfone and Poly (1-Vinylpyrrolidone-Co-Styrene) Copolymers. *J. Membr. Sci.* **2005,** *262(1-2)*, 60-68.

(37) Zhao, G.; Chen, W. N. Biofouling Formation and Structure on Original and Modified Pvdf Membranes: Role of Microbial Species and Membrane Properties. *RSC Adv.* **2017,** *7(60)*, 37990-38000.

(38) Cheng, G.; Li, G.; Xue, H.; Chen, S.; Bryers, J. D.; Jiang, S. Zwitterionic Carboxybetaine Polymer Surfaces and Their Resistance to Long-Term Biofilm Formation. *Biomaterials* **2009,** *30(28)*, 5234-5240.

(39) Cao, B.; Lee, C.-J.; Zeng, Z.; Cheng, F.; Xu, F.; Cong, H.; Cheng, G. Electroactive Poly (Sulfobetaine-3, 4-Ethylenedioxythiophene)(Psbedot) with Controllable Antifouling and Antimicrobial Properties. *Chem. Sci.* **2016,** *7(3)*, 1976-1981.

(40) Ran, F.; Nie, S.; Zhao, W.; Li, J.; Su, B.; Sun, S.; Zhao, C. Biocompatibility of Modified Polyethersulfone Membranes by Blending an Amphiphilic Triblock Co-Polymer of Poly (Vinyl Pyrrolidone)–B-Poly (Methyl Methacrylate)–B-Poly (Vinyl Pyrrolidone). *Acta Biomater.* **2011,** *7(9)*, 3370-3381.

(41) Heydorn, A.; Nielsen, A. T.; Hentzer, M.; Sternberg, C.; Givskov, M.; Ersbøll, B. K.; Molin, S. Quantification of Biofilm Structures by the Novel Computer Program Comstat. *Microbiology* **2000,** *146(10)*, 2395-2407.

(42) Irajizad, P.; Al-Bayati, A.; Eslami, B.; Shafquat, T.; Nazari, M.; Jafari, P.; Kashyap, V.; Masoudi, A.; Araya, D.; Ghasemi, H. Stress-Localized Durable Icephobic Surfaces. *Mater. Horizons* **2019**, 6, 758-766.

(43) Ellinas, K.; Tserepi, A.; Gogolides, E. Durable Superhydrophobic and Superamphiphobic Polymeric Surfaces and Their Applications: A Review. *Adv. Colloid Interface Sci.* **2017,** *250,* 132-157.

(44) Eslami, B.; Irajizad, P.; Jafari, P.; Nazari, M.; Masoudi, A.; Kashyap, V.; Stafslien, S.; Ghasemi, H. Stress-Localized Durable Anti-Biofouling Surfaces. *Soft Matter* **2019,** 15, 6014-6026.

(45) Ghaffarizadeh, S. A.; Zandavi, S. H.; Ward, C. Specific Surface Area from Nitrogen Adsorption Data at 77 K Using the Zeta Adsorption Isotherm. *J. Phys. Chem. C* **2017,** *121(41)*, 23011-23016.

(46) Feng, C.; Zhang, Z.; Li, J.; Qu, Y.; Xing, D.; Gao, X.; Zhang, Z.; Wen, Y.; Ma, Y.; Ye, J. A Bioinspired, Highly Transparent Surface with Dry-Style Antifogging, Antifrosting, Antifouling, and Moisture Self-Cleaning Properties. *Macromol. Rapid Commun.* **2019,** *40(6)*, 1800708.

(47) Nakatani, M.; Shibukawa, A.; Nakagawa, T. Chemical Stability of Polyacrylamide-Coating on Fused Silica Capillary. *Electrophoresis* **1995,** *16(1)*, 1451-1456.

(48) Lakshmi, R.; Bharathidasan, T.; Bera, P.; Basu, B. J. Fabrication of Superhydrophobic and Oleophobic Sol–Gel Nanocomposite Coating. *Surf. Coat. Technol.* **2012,** *206(19-20)*, 3888-3894.

(49) Zhou, H.; Wang, H.; Niu, H.; Fang, J.; Zhao, Y.; Lin, T. Superstrong, Chemically Stable, Superamphiphobic Fabrics from Particle-Free Polymer Coatings. *Adv. Mater. Interfaces* **2015,** *2(6)*, 1400559.

For Table of Contents Only